

# Distributions of Charged Hadrons Associated with High Transverse Momentum Particles in pp and Au+Au Collisions at $\sqrt{s_{NN}}=200$ GeV

J. Adams,<sup>3</sup> C. Adler,<sup>13</sup> M.M. Aggarwal,<sup>27</sup> Z. Ahammed,<sup>40</sup> J. Amonett,<sup>19</sup> B.D. Anderson,<sup>19</sup> D. Arkhipkin,<sup>12</sup>  
G.S. Averichev,<sup>11</sup> S.K. Badyal,<sup>18</sup> J. Balewski,<sup>15</sup> O. Barannikova,<sup>30,11</sup> L.S. Barnby,<sup>3</sup> J. Baudot,<sup>17</sup> S. Bekele,<sup>26</sup>  
V.V. Belaga,<sup>11</sup> R. Bellwied,<sup>43</sup> J. Berger,<sup>13</sup> B.I. Bezverkhny,<sup>45</sup> S. Bhardwaj,<sup>31</sup> A.K. Bhati,<sup>27</sup> H. Bichsel,<sup>42</sup>  
A. Billmeier,<sup>43</sup> L.C. Bland,<sup>2</sup> C.O. Blyth,<sup>3</sup> B.E. Bonner,<sup>32</sup> M. Botje,<sup>25</sup> A. Boucham,<sup>36</sup> A. Brandin,<sup>23</sup> A. Bravar,<sup>2</sup>  
R.V. Cadman,<sup>1</sup> X.Z. Cai,<sup>35</sup> H. Caines,<sup>45</sup> M. Calderón de la Barca Sánchez,<sup>2</sup> J. Carroll,<sup>20</sup> J. Castillo,<sup>20</sup>  
D. Cebra,<sup>5</sup> P. Chaloupka,<sup>10</sup> S. Chattopadhyay,<sup>40</sup> H.F. Chen,<sup>34</sup> Y. Chen,<sup>6</sup> S.P. Chernenko,<sup>11</sup> M. Cherney,<sup>9</sup>  
A. Chikanian,<sup>45</sup> W. Christie,<sup>2</sup> J.P. Coffin,<sup>17</sup> T.M. Cormier,<sup>43</sup> J.G. Cramer,<sup>42</sup> H.J. Crawford,<sup>4</sup> D. Das,<sup>40</sup> S. Das,<sup>40</sup>  
A.A. Derevschikov,<sup>29</sup> L. Didenko,<sup>2</sup> T. Dietel,<sup>13</sup> W.J. Dong,<sup>6</sup> X. Dong,<sup>34,20</sup> J.E. Draper,<sup>5</sup> F. Du,<sup>45</sup> A.K. Dubey,<sup>16</sup>  
V.B. Dunin,<sup>11</sup> J.C. Dunlop,<sup>2</sup> M.R. Dutta Majumdar,<sup>40</sup> V. Eckardt,<sup>21</sup> L.G. Efimov,<sup>11</sup> V. Emelianov,<sup>23</sup> J. Engelage,<sup>4</sup>  
G. Eppley,<sup>32</sup> B. Erazmus,<sup>36</sup> M. Estienne,<sup>36</sup> P. Fachini,<sup>2</sup> V. Faine,<sup>2</sup> J. Faivre,<sup>17</sup> R. Fatemi,<sup>15</sup> K. Filimonov,<sup>20</sup>  
P. Filip,<sup>10</sup> E. Finch,<sup>45</sup> Y. Fisyak,<sup>2</sup> D. Flierl,<sup>13</sup> K.J. Foley,<sup>2</sup> J. Fu,<sup>44</sup> C.A. Gagliardi,<sup>37</sup> N. Gagunashvili,<sup>11</sup>  
J. Gans,<sup>45</sup> M.S. Ganti,<sup>40</sup> L. Gaudichet,<sup>36</sup> F. Geurts,<sup>32</sup> V. Ghazikhanian,<sup>6</sup> P. Ghosh,<sup>40</sup> J.E. Gonzalez,<sup>6</sup>  
O. Grachov,<sup>43</sup> O. Grebenyuk,<sup>25</sup> S. Gronstal,<sup>9</sup> D. Grosnick,<sup>39</sup> S.M. Guertin,<sup>6</sup> A. Gupta,<sup>18</sup> T.D. Gutierrez,<sup>5</sup>  
T.J. Hallman,<sup>2</sup> A. Hamed,<sup>43</sup> D. Hardtke,<sup>20</sup> J.W. Harris,<sup>45</sup> M. Heinz,<sup>45</sup> T.W. Henry,<sup>37</sup> S. Heppelmann,<sup>28</sup>  
T. Herston,<sup>30</sup> B. Hippolyte,<sup>45</sup> A. Hirsch,<sup>30</sup> E. Hjort,<sup>20</sup> G.W. Hoffmann,<sup>38</sup> M. Horsley,<sup>45</sup> H.Z. Huang,<sup>6</sup> S.L. Huang,<sup>34</sup>  
E. Hughes,<sup>7</sup> T.J. Humanic,<sup>26</sup> G. Igo,<sup>6</sup> A. Ishihara,<sup>38</sup> P. Jacobs,<sup>20</sup> W.W. Jacobs,<sup>15</sup> M. Janik,<sup>41</sup> H. Jiang,<sup>6,20</sup>  
I. Johnson,<sup>20</sup> P.G. Jones,<sup>3</sup> E.G. Judd,<sup>4</sup> S. Kabana,<sup>45</sup> M. Kaplan,<sup>8</sup> D. Keane,<sup>19</sup> V.Yu. Khodyrev,<sup>29</sup> J. Kiryluk,<sup>6</sup>  
A. Kisiel,<sup>41</sup> J. Klay,<sup>20</sup> S.R. Klein,<sup>20</sup> A. Klyachko,<sup>15</sup> D.D. Koetke,<sup>39</sup> T. Kollegger,<sup>13</sup> M. Kopytine,<sup>19</sup> L. Kotchenda,<sup>23</sup>  
A.D. Kovalenko,<sup>11</sup> M. Kramer,<sup>24</sup> P. Kravtsov,<sup>23</sup> V.I. Kravtsov,<sup>29</sup> K. Krueger,<sup>1</sup> C. Kuhn,<sup>17</sup> A.I. Kulikov,<sup>11</sup>  
A. Kumar,<sup>27</sup> G.J. Kunde,<sup>45</sup> C.L. Kunz,<sup>8</sup> R.Kh. Kutuev,<sup>12</sup> A.A. Kuznetsov,<sup>11</sup> M.A.C. Lamont,<sup>3</sup> J.M. Landgraf,<sup>2</sup>  
S. Lange,<sup>13</sup> B. Lasiuk,<sup>45</sup> F. Laue,<sup>2</sup> J. Lauret,<sup>2</sup> A. Lebedev,<sup>2</sup> R. Lednický,<sup>11</sup> M.J. LeVine,<sup>2</sup> C. Li,<sup>34</sup> Q. Li,<sup>43</sup>  
S.J. Lindenbaum,<sup>24</sup> M.A. Lisa,<sup>26</sup> F. Liu,<sup>44</sup> L. Liu,<sup>44</sup> Z. Liu,<sup>44</sup> Q.J. Liu,<sup>42</sup> T. Ljubicic,<sup>2</sup> W.J. Llope,<sup>32</sup> H. Long,<sup>6</sup>  
R.S. Longacre,<sup>2</sup> M. Lopez-Noriega,<sup>26</sup> W.A. Love,<sup>2</sup> T. Ludlam,<sup>2</sup> D. Lynn,<sup>2</sup> J. Ma,<sup>6</sup> Y.G. Ma,<sup>35</sup> D. Magestro,<sup>26</sup>  
S. Mahajan,<sup>18</sup> L.K. Mangotra,<sup>18</sup> D.P. Mahapatra,<sup>16</sup> R. Majka,<sup>45</sup> R. Manweiler,<sup>39</sup> S. Margetis,<sup>19</sup> C. Markert,<sup>45</sup>  
L. Martin,<sup>36</sup> J. Marx,<sup>20</sup> H.S. Matis,<sup>20</sup> Yu.A. Matulenko,<sup>29</sup> C.J. McClain,<sup>1</sup> T.S. McShane,<sup>9</sup> F. Meissner,<sup>20</sup>  
Yu. Melnick,<sup>29</sup> A. Meschanin,<sup>29</sup> M.L. Miller,<sup>45</sup> Z. Milosevich,<sup>8</sup> N.G. Minaev,<sup>29</sup> C. Mironov,<sup>19</sup> A. Mischke,<sup>25</sup>  
D. Mishra,<sup>16</sup> J. Mitchell,<sup>32</sup> B. Mohanty,<sup>40</sup> L. Molnar,<sup>30</sup> C.F. Moore,<sup>38</sup> M.J. Mora-Corral,<sup>21</sup> D.A. Morozov,<sup>29</sup>  
V. Morozov,<sup>20</sup> M.M. de Moura,<sup>33</sup> M.G. Munhoz,<sup>33</sup> B.K. Nandi,<sup>40</sup> S.K. Nayak,<sup>18</sup> T.K. Nayak,<sup>40</sup> J.M. Nelson,<sup>3</sup>  
P.K. Netrakanti,<sup>40</sup> V.A. Nikitin,<sup>12</sup> L.V. Nogach,<sup>29</sup> B. Norman,<sup>19</sup> S.B. Nurushev,<sup>29</sup> G. Odyniec,<sup>20</sup> A. Ogawa,<sup>2</sup>  
V. Okorokov,<sup>23</sup> M. Oldenburg,<sup>20</sup> D. Olson,<sup>20</sup> G. Paic,<sup>26</sup> S.K. Pal,<sup>40</sup> Y. Panebratsev,<sup>11</sup> S.Y. Panitkin,<sup>2</sup>  
A.I. Pavlinov,<sup>43</sup> T. Pawlak,<sup>41</sup> T. Peitzmann,<sup>25</sup> V. Perevoztchikov,<sup>2</sup> C. Perkins,<sup>4</sup> W. Peryt,<sup>41</sup> V.A. Petrov,<sup>12</sup>  
S.C. Phatak,<sup>16</sup> R. Picha,<sup>5</sup> M. Planinic,<sup>46</sup> J. Pluta,<sup>41</sup> N. Porile,<sup>30</sup> J. Porter,<sup>2</sup> A.M. Poskanzer,<sup>20</sup> M. Potekhin,<sup>2</sup>  
E. Potrebenikova,<sup>11</sup> B.V.K.S. Potukuchi,<sup>18</sup> D. Prindle,<sup>42</sup> C. Pruneau,<sup>43</sup> J. Putschke,<sup>21</sup> G. Rai,<sup>20</sup> G. Rakness,<sup>15</sup>  
R. Raniwala,<sup>31</sup> S. Raniwala,<sup>31</sup> O. Ravel,<sup>36</sup> R.L. Ray,<sup>38</sup> S.V. Razin,<sup>11,15</sup> D. Reichhold,<sup>30</sup> J.G. Reid,<sup>42</sup> G. Renault,<sup>36</sup>  
F. Retiere,<sup>20</sup> A. Ridiger,<sup>23</sup> H.G. Ritter,<sup>20</sup> J.B. Roberts,<sup>32</sup> O.V. Rogachevski,<sup>11</sup> J.L. Romero,<sup>5</sup> A. Rose,<sup>43</sup> C. Roy,<sup>36</sup>  
L.J. Ruan,<sup>34,2</sup> R. Sahoo,<sup>16</sup> I. Sakrejda,<sup>20</sup> S. Salur,<sup>45</sup> J. Sandweiss,<sup>45</sup> I. Savin,<sup>12</sup> J. Schambach,<sup>38</sup> R.P. Scharenberg,<sup>30</sup>  
N. Schmitz,<sup>21</sup> L.S. Schroeder,<sup>20</sup> K. Schweda,<sup>20</sup> J. Seger,<sup>9</sup> P. Seyboth,<sup>21</sup> E. Shabaliev,<sup>11</sup> M. Shao,<sup>34</sup> W. Shao,<sup>7</sup>  
M. Sharma,<sup>27</sup> K.E. Shestermanov,<sup>29</sup> S.S. Shimanskii,<sup>11</sup> R.N. Singaraju,<sup>40</sup> F. Simon,<sup>21</sup> G. Skoro,<sup>11</sup> N. Smirnov,<sup>45</sup>  
R. Snellings,<sup>25</sup> G. Sood,<sup>27</sup> P. Sorensen,<sup>20</sup> J. Sowinski,<sup>15</sup> J. Speltz,<sup>17</sup> H.M. Spinka,<sup>1</sup> B. Srivastava,<sup>30</sup>  
T.D.S. Stanislaus,<sup>39</sup> R. Stock,<sup>13</sup> A. Stolpovsky,<sup>43</sup> M. Strikhanov,<sup>23</sup> B. Stringfellow,<sup>30</sup> C. Struck,<sup>13</sup> A.A.P. Suaide,<sup>33</sup>  
E. Sugarbaker,<sup>26</sup> C. Suire,<sup>2</sup> M. Šumbera,<sup>10</sup> B. Surrow,<sup>2</sup> T.J.M. Symons,<sup>20</sup> A. Szanto de Toledo,<sup>33</sup> P. Szarwas,<sup>41</sup>  
A. Tai,<sup>6</sup> J. Takahashi,<sup>33</sup> A.H. Tang,<sup>2,25</sup> D. Thein,<sup>6</sup> J.H. Thomas,<sup>20</sup> S. Timoshenko,<sup>23</sup> M. Tokarev,<sup>11</sup> M.B. Tonjes,<sup>22</sup>  
T.A. Trainor,<sup>42</sup> S. Trentalange,<sup>6</sup> R.E. Tribble,<sup>37</sup> O. Tsai,<sup>6</sup> T. Ullrich,<sup>2</sup> D.G. Underwood,<sup>1</sup> G. Van Buren,<sup>2</sup>  
A.M. VanderMolen,<sup>22</sup> R. Varma,<sup>14</sup> I. Vasilevski,<sup>12</sup> A.N. Vasiliev,<sup>29</sup> R. Vernet,<sup>17</sup> S.E. Vigdor,<sup>15</sup> Y.P. Viyogi,<sup>40</sup>  
S.A. Voloshin,<sup>43</sup> M. Vznuzdaev,<sup>23</sup> W. Wagoner,<sup>9</sup> F. Wang,<sup>30</sup> G. Wang,<sup>7</sup> G. Wang,<sup>19</sup> X.L. Wang,<sup>34</sup> Y. Wang,<sup>38</sup>  
Z.M. Wang,<sup>34</sup> H. Ward,<sup>38</sup> J.W. Watson,<sup>19</sup> J.C. Webb,<sup>15</sup> R. Wells,<sup>26</sup> G.D. Westfall,<sup>22</sup> C. Whitten Jr.,<sup>6</sup> H. Wieman,<sup>20</sup>  
R. Willson,<sup>26</sup> S.W. Wissink,<sup>15</sup> R. Witt,<sup>45</sup> J. Wood,<sup>6</sup> J. Wu,<sup>34</sup> N. Xu,<sup>20</sup> Z. Xu,<sup>2</sup> Z.Z. Xu,<sup>34</sup> E. Yamamoto,<sup>20</sup>  
P. Yepes,<sup>32</sup> V.I. Yurevich,<sup>11</sup> B. Yuting,<sup>25</sup> Y.V. Zanevski,<sup>11</sup> H. Zhang,<sup>45,2</sup> W.M. Zhang,<sup>19</sup> Z.P. Zhang,<sup>34</sup>

Z.P. Zhaomin,<sup>34</sup> Z.P. Zizong,<sup>34</sup> P.A. Żołnierczuk,<sup>15</sup> R. Zoukarneev,<sup>12</sup> J. Zoukarneeva,<sup>12</sup> and A.N. Zubarev<sup>11</sup>  
(STAR Collaboration),\*

- <sup>1</sup>Argonne National Laboratory, Argonne, Illinois 60439  
<sup>2</sup>Brookhaven National Laboratory, Upton, New York 11973  
<sup>3</sup>University of Birmingham, Birmingham, United Kingdom  
<sup>4</sup>University of California, Berkeley, California 94720  
<sup>5</sup>University of California, Davis, California 95616  
<sup>6</sup>University of California, Los Angeles, California 90095  
<sup>7</sup>California Institute of Technology, Pasadena, California 91125  
<sup>8</sup>Carnegie Mellon University, Pittsburgh, Pennsylvania 15213  
<sup>9</sup>Creighton University, Omaha, Nebraska 68178  
<sup>10</sup>Nuclear Physics Institute AS CR, Řež/Prague, Czech Republic  
<sup>11</sup>Laboratory for High Energy (JINR), Dubna, Russia  
<sup>12</sup>Particle Physics Laboratory (JINR), Dubna, Russia  
<sup>13</sup>University of Frankfurt, Frankfurt, Germany  
<sup>14</sup>Indian Institute of Technology, Mumbai, India  
<sup>15</sup>Indiana University, Bloomington, Indiana 47408  
<sup>16</sup>Institute of Physics, Bhubaneswar 751005, India  
<sup>17</sup>Institut de Recherches Subatomiques, Strasbourg, France  
<sup>18</sup>University of Jammu, Jammu 180001, India  
<sup>19</sup>Kent State University, Kent, Ohio 44242  
<sup>20</sup>Lawrence Berkeley National Laboratory, Berkeley, California 94720  
<sup>21</sup>Max-Planck-Institut für Physik, Munich, Germany  
<sup>22</sup>Michigan State University, East Lansing, Michigan 48824  
<sup>23</sup>Moscow Engineering Physics Institute, Moscow Russia  
<sup>24</sup>City College of New York, New York City, New York 10031  
<sup>25</sup>NIKHEF, Amsterdam, The Netherlands  
<sup>26</sup>Ohio State University, Columbus, Ohio 43210  
<sup>27</sup>Panjab University, Chandigarh 160014, India  
<sup>28</sup>Pennsylvania State University, University Park, Pennsylvania 16802  
<sup>29</sup>Institute of High Energy Physics, Protvino, Russia  
<sup>30</sup>Purdue University, West Lafayette, Indiana 47907  
<sup>31</sup>University of Rajasthan, Jaipur 302004, India  
<sup>32</sup>Rice University, Houston, Texas 77251  
<sup>33</sup>Universidade de Sao Paulo, Sao Paulo, Brazil  
<sup>34</sup>University of Science & Technology of China, Anhui 230027, China  
<sup>35</sup>Shanghai Institute of Nuclear Research, Shanghai 201800, P.R. China  
<sup>36</sup>SUBATECH, Nantes, France  
<sup>37</sup>Texas A&M University, College Station, Texas 77843  
<sup>38</sup>University of Texas, Austin, Texas 78712  
<sup>39</sup>Valparaiso University, Valparaiso, Indiana 46383  
<sup>40</sup>Variable Energy Cyclotron Centre, Kolkata 700064, India  
<sup>41</sup>Warsaw University of Technology, Warsaw, Poland  
<sup>42</sup>University of Washington, Seattle, Washington 98195  
<sup>43</sup>Wayne State University, Detroit, Michigan 48201  
<sup>44</sup>Institute of Particle Physics, CCNU (HZNU), Wuhan, 430079 China  
<sup>45</sup>Yale University, New Haven, Connecticut 06520  
<sup>46</sup>University of Zagreb, Zagreb, HR-10002, Croatia

Charged hadrons in  $0.15 < p_{\perp} < 4$  GeV/c associated with particles of  $p_{\perp}^{\text{trig}} > 4$  GeV/c are reconstructed in pp and Au+Au collisions at  $\sqrt{s_{\text{NN}}} = 200$  GeV. The associated multiplicity and  $p_{\perp}$  magnitude sum are found to increase from pp to central Au+Au collisions. The associated  $p_{\perp}$  distributions, while similar in shape on the near side, are significantly softened on the away side in central Au+Au relative to pp and not much harder than that of inclusive hadrons. The results, consistent with jet quenching, suggest that the away-side fragments approach equilibration with the medium traversed.

PACS numbers: 25.75.-q, 25.75.Dw

*Introduction*—Quantum Chromodynamics (QCD) predicts a phase transition between hadronic matter and quark-gluon plasma at a critical energy density of  $\sim 1$  GeV/fm<sup>3</sup> [1]. Such a phase transition is being actively

pursued at the Relativistic Heavy-Ion Collider (RHIC). High transverse momentum ( $p_{\perp}$ ) particles, emerging from hard-scatterings, lose energy while traversing and interacting with the medium being developed in heavy-

ion collisions. Energy loss results in jet quenching [2] – suppressions of hadron yield and back-to-back angular correlation strength at high  $p_{\perp}$ . Such suppressions were observed in central Au+Au collisions at RHIC [3, 4] and attributed to final-state interactions when no suppression was seen in d+Au [5]. Perturbative QCD model calculations invoking parton energy loss require 30 times the normal nuclear gluon density in order to account for the central Au+Au results [6].

The depleted energy at high  $p_{\perp}$  must be redistributed to low  $p_{\perp}$  particles [7]. Reconstruction of these particles will constrain models describing production mechanisms of high  $p_{\perp}$  particles, and may shed light on the underlying energy loss mechanism(s) and the degree of equilibration of jet products with the medium.

This Letter presents results from a statistical reconstruction, via two-particle angular correlations, of charged hadrons in  $0.15 < p_{\perp} < 4$  GeV/c associated with a high  $p_{\perp}$  “trigger” particle in pp and Au+Au collisions at  $\sqrt{s_{NN}}=200$  GeV. Two  $p_{\perp}$  windows for trigger particles,  $4 < p_{\perp}^{\text{trig}} < 6$  GeV/c and  $6 < p_{\perp}^{\text{trig}} < 10$  GeV/c, are presented. The latter range is expected [8, 9] to provide a purer, though much lower statistics, sample of hard scattering products. Results are reported as a function of centrality for Au+Au collisions and the associated hadron  $p_{\perp}$ .

*Analysis*– The STAR experiment [10] is well suited for this measurement due to significant pseudo-rapidity ( $\eta$ ) and complete azimuthal ( $\phi$ ) coverage. The STAR Time Projection Chamber (TPC) resides in a magnetic field of 0.5 T along its cylindrical axis (= the beam direction). Events with reconstructed primary vertex within  $\pm 25$  cm longitudinally of the TPC center are used. The Au+Au events are divided into 7 centrality classes as in [4].

High  $p_{\perp}$  trigger particles are selected with  $|\eta_{\text{trig}}| < 0.7$  and  $dca < 1$  cm ( $dca$  = distance of closest approach to the primary vertex). Other particles in the event with  $|\eta| < 1.0$  and  $dca < 2$  cm are paired with each trigger particle to form  $\Delta\eta = \eta - \eta_{\text{trig}}$  and  $\Delta\phi = \phi - \phi_{\text{trig}}$  distributions. The primary vertex was included in the momentum fit of the associated particles, but not for trigger particles to minimize weak decay background.

Combinatorial coincidences are removed from the measured angular correlations by subtracting mixed-event background of the same centrality bin, so that detector non-uniformities should affect signal and background distributions in the same way. The effect of elliptic flow ( $v_2$ ) is included by multiplying the Au+Au mixed-event background by  $1 + 2v_2(p_{\perp}^{\text{trig}})v_2(p_{\perp}) \cos(2\Delta\phi)$  [11]. The mixed (minimum-bias trigger) events may not precisely match the underlying background in events with a trigger particle, e.g., due to different centrality distributions within each analyzed bin. Hence, an additional  $p_{\perp}$ -independent factor (1.46 for pp and 0.995-1.000 for Au+Au) has been applied to the background before subtraction, in order to normalize it to the measured  $\Delta\phi$  distribution within

$0.8 < |\Delta\phi| < 1.2$  for  $0.15 < p_{\perp} < 4$  GeV/c.

Figure 1 shows the background subtracted  $\Delta\phi$  ( $|\eta| < 1.0$ ) and  $\Delta\eta$  ( $|\Delta\phi| < 0.5$  or  $|\Delta\phi - \pi| < 1.0$ ) distributions in pp and central Au+Au collisions. The distributions are corrected for single particle acceptance and efficiency and are normalized per trigger particle. The  $\Delta\eta$  distributions are further corrected for two-particle acceptance. We refer to the ( $|\Delta\phi| < 1.0$ ,  $|\Delta\eta| < 1.4$ ) region as near side and to the ( $|\Delta\phi| > 1.0$ ,  $|\eta| < 1.0$ ) region as away side. On the near side, correlation structures typical of jets are observed in pp and Au+Au collisions; the  $\Delta\eta$  distribution is broader in central Au+Au than in pp collisions, while the  $\Delta\phi$  distributions are similar in shape. On the away side, the  $\Delta\eta$  distributions are flat within the measured range of  $|\Delta\eta| < 1.4$ , and the  $\Delta\phi$  distribution is broader in central Au+Au than in pp collisions. The correlation signal in central Au+Au is stronger than in pp on the near side; that on the away side is stronger at low  $p_{\perp}$ , and weaker at high  $p_{\perp}$ , qualitatively consistent with results in [4].

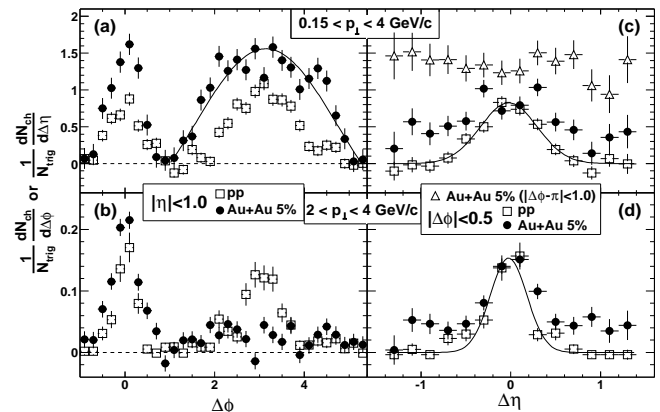


FIG. 1: Background subtracted (a-b)  $\Delta\phi$  and (c-d)  $\Delta\eta$  distributions for pp and 5-0% central Au+Au collisions for  $4 < p_{\perp}^{\text{trig}} < 6$  GeV/c and two associated  $p_{\perp}$  ranges. The subtracted background level is  $\frac{1}{N_{\text{trig}}} \frac{dN_{\text{ch}}}{d\Delta\phi} \approx 1.4$  (0.007) in pp and  $\approx 211$  (2.1) in 5-0% Au+Au events for  $0.15 < p_{\perp} < 4$  GeV/c ( $2 < p_{\perp} < 4$  GeV/c). The curve in (a) shows the shape of an  $[A - B \cos(\Delta\phi)]$  function. The curves in (c-d) are Gaussian fits to the pp data.

We integrate the correlation peaks as measures of associated charged hadron multiplicities ( $\mathcal{N}_{\text{ch}}$ ). We obtain  $p_{\perp}$  magnitude sum ( $\mathcal{P}_{\perp}$ ), which approximates associated energy, and total vector  $\vec{\mathcal{P}}_{\perp}$  from the  $p_{\perp}$ -weighted  $\Delta\phi$  and  $\Delta\eta$  distributions multiplied by  $1.58 \pm 0.08$  [12] to account for the undetected neutrals. The trigger particle  $p_{\perp}^{\text{trig}}$  is then included in  $\mathcal{P}_{\perp}$  and  $\vec{\mathcal{P}}_{\perp}$  for the near side.

*Systematic uncertainties*– Table I lists the major sources of systematic uncertainties in  $\mathcal{N}_{\text{ch}}$ . (1) Uncertainty in acceptance and efficiency correction is estimated to be 10%. (2) In constructing background, we use the average of the  $v_2$  results from the modified reaction plane ( $v_2\{\text{MRP}\}$ ) [13] and the 4-particle ( $v_2\{4\}$ ) [14] methods and assign the resulting difference as uncertainty. For the

80-60% and 5-0% centralities where  $v_2\{4\}$  are unavailable, we estimate  $v_2\{4\} \approx v_2\{\text{MRP}\}/2$ . Relatively small uncertainties arise on the away side because the  $\Delta\phi$  integration range is much broader than  $\pi/2$  and the background normalization is correlated with the  $v_2$  correction used. (3) Uncertainties in background normalization for  $0.15 < p_\perp < 4$  GeV/c are estimated by varying the  $\Delta\phi$  region for normalization. (4) An additional (single-sided) uncertainty due to possible  $p_\perp$ -dependent differences between the mixed-event and true background is estimated by comparing to results using  $p_\perp$ -dependent background normalization. The systematic errors from the above sources are added in quadrature, separately for the positive and negative uncertainties.

TABLE I: Major sources of systematic uncertainties (in percent) in  $\mathcal{N}_{\text{ch}}$  for  $4 < p_\perp^{\text{trig}} < 6$  GeV/c.

source	pp		80-60%	30-20%	5-0%				
	near	away	near	away	near	away			
(1) effc.	$\pm 10$		$\pm 10$	$\pm 10$	$\pm 10$				
(2) flow	-		+34 -40	$\pm 4$	+21 -22	$\pm 5$	+19 -27	+4 -5	
(3) bkgd.	+22 -13	+22 -14	+62 -6	+36 -4	+27 -12	+32 -14	+11 -14	+10 -13	
(4) $p_\perp$ - dep.	$p_\perp$ (GeV/c)		pp		80-40%		5-0%		
	near	away	near	away	near	away	near	away	
	0.5-1.0		+1	-7	-39	-6	-5	+1	
	1.5-2.0		-25	-29	-28	-25	+7	+7	
		2.5-3.0		-1	-16	-9	-16	-6	-15

*Results*– Figure 2 shows  $\mathcal{N}_{\text{ch}}$  and  $\mathcal{P}_\perp$  in pp and as a function of centrality (the charged hadron  $dN_{\text{ch}}/d\eta$ ) in Au+Au collisions for the two  $p_\perp^{\text{trig}}$  windows of 4-6 GeV/c and 6-10 GeV/c. The trigger particle is not included in  $\mathcal{N}_{\text{ch}}$  and is included in  $\mathcal{P}_\perp$  for the near side. For pp and all centralities of Au+Au,  $\langle p_\perp^{\text{trig}} \rangle \approx 4.55$  GeV/c and 7.0 GeV/c for the two  $p_\perp^{\text{trig}}$  windows, respectively. With the same  $\langle p_\perp^{\text{trig}} \rangle$  trigger particle,  $\mathcal{N}_{\text{ch}}$  and  $\mathcal{P}_\perp$  increase from pp to central Au+Au collisions for both the near and away sides, and for both  $p_\perp^{\text{trig}}$  selections.

Our results include nearly all associated hadrons on the near side, but only the fraction within our acceptance on the away side. We find the  $\vec{\mathcal{P}}_\perp$  ratio of away side to near side  $\approx 40\%$ , independent of collision system or centrality. This may reflect the TPC acceptance for away side associated hadrons because  $\vec{\mathcal{P}}_\perp$  of the entire event has to be balanced.

Figure 3(a-b) shows the  $p_\perp$  distributions of associated charged hadrons for  $4 < p_\perp^{\text{trig}} < 6$  GeV/c in pp, peripheral 80-40% and central 5-0% Au+Au collisions. The Au+Au to pp spectra ratios (AA/pp) are depicted in Fig. 3(c-d). Results for peripheral Au+Au generally agree with pp, while those for central Au+Au differ. On the near side, the spectral shapes are similar within errors, while the associated multiplicity is larger in central Au+Au col-

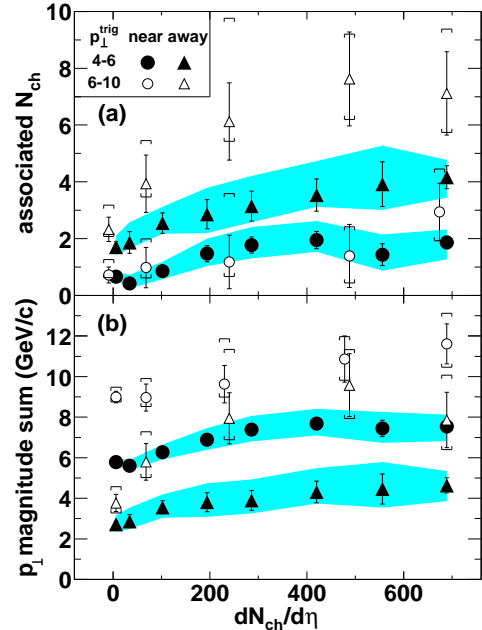


FIG. 2: (a)  $\mathcal{N}_{\text{ch}}$  and (b)  $\mathcal{P}_\perp$  for  $4 < p_\perp^{\text{trig}} < 6$  GeV/c (systematic errors in bands) and  $6 < p_\perp^{\text{trig}} < 10$  GeV/c (systematic errors in caps). The leftmost set of data are for pp. Some of the open points are slightly displaced in  $dN_{\text{ch}}/d\eta$  for clarity. The systematic errors are strongly correlated between the near and away side and among the centralities.

lisions than in pp. On the away side, the spectrum is significantly softened in central Au+Au collisions; associated particles are depleted at high  $p_\perp$ , as first noted in [4], and are significantly enhanced at low  $p_\perp$ .

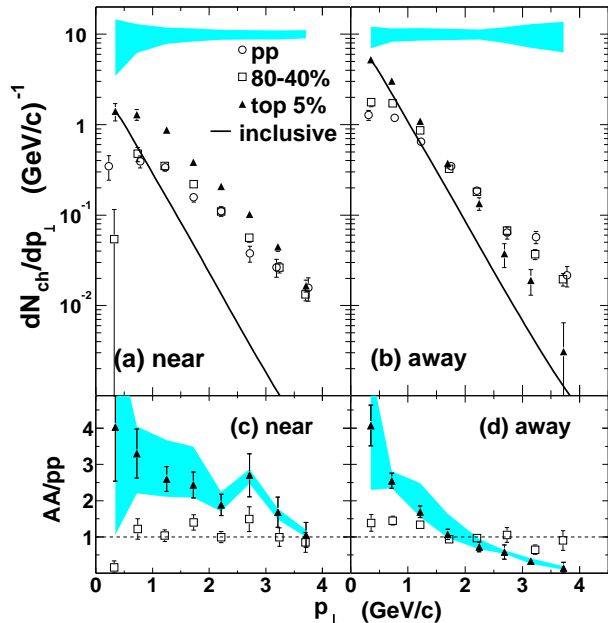
Table II lists the AA/pp ratios of integrated yields over  $0.15 < p_\perp < 4$  GeV/c and  $2 < p_\perp < 4$  GeV/c. In the systematic uncertainties for AA/pp, sources (1), (3), and (4) in Table I tend to cancel. AA/pp is consistent with unity for peripheral collisions; it deviates significantly for central collisions: the AA signal is much stronger on the near side, much stronger (and broader) at low  $p_\perp$  and suppressed and broadened at high  $p_\perp$  on the away side.

Table II also lists the analogous measure  $I_{AA}$  for  $2 < p_\perp < 4$  GeV/c, extracted in the present analysis following the procedure established in [4]. The present  $I_{AA}$  differ from those in [4] primarily due to use of reduced  $v_2$  values and a more stringent primary vertex cut for pp. The systematic errors quoted for  $I_{AA}$  are from  $v_2$  and background uncertainties, the latter estimated by fitting to different  $\Delta\phi$  ranges besides the default  $0.75 < \Delta\phi < 2.24$ . While they exhibit similar trends,  $I_{AA}$  and AA/pp differ quantitatively due to differences in integration ranges and methodology: e.g., the  $I_{AA}$  prescription omits two-particle acceptance corrections, and thereby suppresses long-range  $\Delta\eta$  correlation signals which may contribute to AA/pp after mixed-event and elliptic flow subtraction.

Figure 4 shows the centrality dependence of  $\langle p_\perp \rangle$  of the

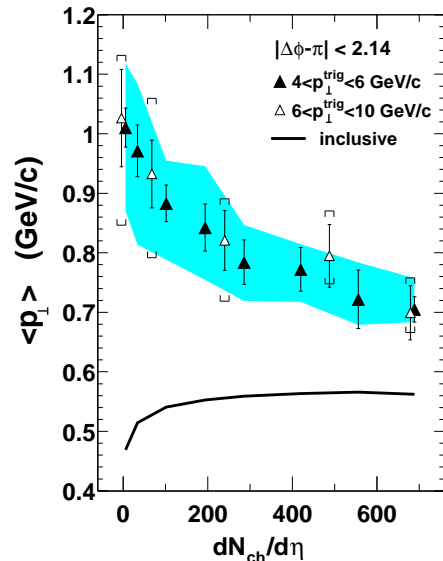
TABLE II: AA/pp and  $I_{AA}$  of  $p_{\perp}$ -integrated yields for  $4 < p_{\perp}^{\text{trig}} < 6$  GeV/c. The first error is statistical and the second systematic.

	$p_{\perp}$ (GeV/c)	80-60% near	80-60% away	5-0% near	5-0% away
AA/pp	0.15-4.0	$0.64 \pm 0.25^{+0.30}_{-0.26}$	$1.10 \pm 0.26^{+0.14}_{-0.13}$	$2.81 \pm 0.50^{+0.55}_{-0.80}$	$2.45 \pm 0.36^{+0.09}_{-0.26}$
	2.0-4.0	$1.04 \pm 0.13^{+0.06}_{-0.09}$	$0.85 \pm 0.11 \pm 0.04$	$1.95 \pm 0.11^{+0.17}_{-0.13}$	$0.59 \pm 0.14^{+0.09}_{-0.04}$
$I_{AA}$	2.0-4.0	$0.99 \pm 0.11^{+0.06}_{-0.08}$	$0.85 \pm 0.09^{+0.05}_{-0.07}$	$1.55 \pm 0.14^{+0.13}_{-0.17}$	$0.28 \pm 0.06^{+0.10}_{-0.14}$


 FIG. 3: Associated charged hadron  $p_{\perp}$  distributions (a-b) and AA/pp ratios (c-d) for  $4 < p_{\perp}^{\text{trig}} < 6$  GeV/c on near and away side. Errors shown are statistical. The bands show the systematic uncertainties for the 5-0% central data. The lines show the inclusive spectral shape for central collisions.

away side associated particles. Also shown by the line are the  $\langle p_{\perp} \rangle$  of inclusive hadrons. The associated particle  $\langle p_{\perp} \rangle$ , while significantly larger than that of inclusive hadrons in pp and peripheral Au+Au collisions, drops rapidly with centrality in Au+Au collisions, approaching the inclusive hadron  $\langle p_{\perp} \rangle$ . The features are similar for the two  $p_{\perp}^{\text{trig}}$  selections. The results may indicate a progressive equilibration of the associated hadrons with the bulk medium from peripheral to central collisions.

*Discussion*– High  $p_{\perp}$  particles in pp and peripheral Au+Au collisions are predominantly from hard scatterings and jets [2]. The production mechanisms of high  $p_{\perp}$  particles in central Au+Au collisions are less understood. A non-negligible fraction of the trigger particles in  $4 < p_{\perp}^{\text{trig}} < 6$  GeV/c may come from mechanisms other than pure parton fragmentation [8, 9]. Such softer contributions are expected to be negligible in the  $6 < p_{\perp}^{\text{trig}} < 10$  GeV/c region. The qualitative consistency between the two  $p_{\perp}^{\text{trig}}$  windows thus suggests that they reflect features of hard scattering in Au+Au collisions.


 FIG. 4: Away side associated charged hadron  $\langle p_{\perp} \rangle$  for  $4 < p_{\perp}^{\text{trig}} < 6$  GeV/c (systematic errors in band) and  $6 < p_{\perp}^{\text{trig}} < 10$  GeV/c (systematic errors in caps). The leftmost set of data are for pp. Some of the open points are slightly displaced in  $dN_{\text{ch}}/d\eta$  for clarity.

In the context of di-jet production and subsequent energy loss, high  $p_{\perp}^{\text{trig}}$  particles select preferentially di-jets produced near the medium surface [4]. The near side jet traverses and interacts with a minimal amount of matter. No broadening is observed in the  $\Delta\phi$  correlation. The observed broadening in  $\Delta\eta$  is possibly due to transverse radial flow and/or longitudinal expansion of the medium [15]. More hadrons and larger energy accompany the same  $\langle p_{\perp}^{\text{trig}} \rangle$  trigger particle in central Au+Au collisions than in pp. This could be the net effect of modest parton energy loss and energy pickup from the medium through coalescence/recombination processes [9], resulting in no significant changes in spectral shape.

The away side jet traverses a large amount of matter. Significant energy loss occurs resulting in a large depletion of high  $p_{\perp}$  fragments and an enhancement at low  $p_{\perp}$ : energy transferred from high to low  $p_{\perp}$  results in an increase in the total associated hadron multiplicity. Given the limited TPC acceptance for away jets, our results indicate a large difference between pp and central Au+Au collisions; a significant amount of associated energy may come from the medium in central collisions. The final remnants in central Au+Au collisions no longer

exhibit jet-like angular correlations. The  $\Delta\phi$  distribution is broadened, and seems to have reached the limit prescribed statistically by momentum balance [16] (see the curve superimposed in Fig. 1a). The interactions seem to have driven particles from the two sources, jet fragmentation and the bulk medium, to approach equilibration. This may in turn imply a high degree of thermalization within the medium itself.

*Conclusions*– We have reported results on statistical reconstruction, via two-particle angular correlations, of charged hadrons in  $0.15 < p_{\perp} < 4$  GeV/c associated with particles of  $p_{\perp}^{\text{trig}} > 4$  GeV/c in pp and Au+Au collisions at RHIC. It is found, with the same  $\langle p_{\perp}^{\text{trig}} \rangle$  trigger particle in the final state, that associated hadron multiplicity and  $p_{\perp}$  magnitude sum increase from pp to central Au+Au collisions. The transverse momentum distributions of associated hadrons, while similar in shape on the near side, are found to be significantly softened on the away side in central Au+Au collisions relative to pp. The average  $p_{\perp}$  of the away side associated hadrons decreases with centrality, and becomes not much larger than that of inclusive hadrons, indicating a progressive equilibration between the away side associated hadrons and the medium. The results are qualitatively the same for  $4 < p_{\perp}^{\text{trig}} < 6$  GeV/c and  $6 < p_{\perp}^{\text{trig}} < 10$  GeV/c, and are qualitatively consistent with modification of jets in heavy-ion collisions at RHIC.

We thank the RHIC Operations Group and RCF at BNL, and the NERSC Center at LBNL for their support. This work was supported in part by the HENP Divisions of the Office of Science of the U.S. DOE; the U.S. NSF; the BMBF of Germany; IN2P3, RA, RPL, and EMN of France; EPSRC of the United Kingdom; FAPESP of Brazil; the Russian Ministry of Science and Technology; the Ministry of Education and the NNSFC of China; Grant Agency of the Czech Republic, FOM and UU of the Netherlands, DAE, DST, and CSIR of the Government of India; the Swiss NSF.

- [1] F. Karsch, Nucl. Phys. **A698**, 199c (2002).
- [2] M. Gyulassy and M. Plümer, Phys. Lett. B **243**, 432 (1990); X.-N. Wang and M. Gyulassy, Phys. Rev. Lett. **68**, 1480 (1992); R. Baier, D. Schiff, and B.G. Zakharov, Ann. Rev. Nucl. Part. Sci. **50**, 37 (2000).
- [3] K. Adcox *et al.* (PHENIX), Phys. Rev. Lett. **88**, 022301 (2002); C. Adler *et al.* (STAR), Phys. Rev. Lett. **89**, 202301 (2002); S.S. Adler *et al.* (PHENIX), Phys. Rev. Lett. **91**, 072301 (2003); J. Adams *et al.* (STAR), Phys. Rev. Lett. **91**, 172302 (2003).
- [4] C. Adler *et al.* (STAR), Phys. Rev. Lett. **90**, 082302 (2003).
- [5] B.B. Back *et al.* (PHOBOS), Phys. Rev. Lett. **91**, 072302 (2003); S.S. Adler *et al.* (PHENIX), Phys. Rev. Lett. **91**, 072303 (2003); J. Adams *et al.* (STAR), Phys. Rev. Lett. **91**, 072304 (2003); I. Arsene *et al.* (BRAHMS), Phys. Rev. Lett. **91**, 072305 (2003).
- [6] I. Vitev and M. Gyulassy, Phys. Rev. Lett. **89**, 252301 (2002); X.-N. Wang, Phys. Lett. B **595**, 165 (2004).
- [7] S. Pal and S. Pratt, Phys. Lett. B **574**, 21 (2003); X.-N. Wang, Phys. Lett. B **579**, 299 (2004); C.A. Salgado and U.A. Wiedemann, Phys. Rev. Lett. **93**, 042301 (2004).
- [8] V. Greco, C.M. Ko, and P. Levai, Phys. Rev. **C68**, 034904 (2003); R.J. Fries *et al.*, Phys. Rev. **C68**, 044902 (2003).
- [9] R.C. Hwa and C.B. Yang, Phys. Rev. **C70**, 024905 (2004).
- [10] K.H. Ackermann *et al.* (STAR), Nucl. Instrum. Meth. **A499**, 624 (2003).
- [11] C. Adler *et al.* (STAR), Phys. Rev. Lett. **90**, 032301 (2003); J. Adams *et al.* (STAR), Phys. Rev. Lett. **93**, 252301 (2004).
- [12] J. Adams *et al.* (STAR), Phys. Rev. Lett. **92**, 112301 (2004); S.S. Adler *et al.* (PHENIX), Phys. Rev. **C69**, 034909 (2004). Assuming isospin symmetry, the ratio of total to charged hadron multiplicity  $\approx 1.58$ . PYTHIA and HIJING models indicate a ratio of 1.60-1.65 for jet fragments with charged trigger particle of  $p_{\perp}^{\text{trig}} > 4$  GeV/c.
- [13] J. Adams *et al.* (STAR), nucl-ex/0409033.
- [14] C. Adler *et al.* (STAR), Phys. Rev. **C66**, 034904 (2002).
- [15] S.A. Voloshin, nucl-th/0312065; N. Armesto, C.A. Salgado, and U.A. Wiedemann, Phys. Rev. Lett. **93**, 242301 (2004).
- [16] N. Borghini, P.M. Dinh, and J-Y Ollitrault, Phys. Rev. **C62**, 034902 (2000).

---

\* URL: [www.star.bnl.gov](http://www.star.bnl.gov)